Available online at www.sciencedirect.com
SCIENCE DIRECT®
Thin Solid Films 451–452 (2004) 536–543
thin solid films
www.elsevier.com/locate/tsf

Stability aspects in CdTe/CdS solar cells

D.L. Bätzner[a], A. Romeo[a], M. Terheggen[b], M. Döbeli[c], H. Zogg[a], A.N. Tiwari[a,d,*]

[a]*Thin Film Physics Group, Laboratory for Solid State Physics, ETH Zürich, Technoparkstrasse 1, 8005 Zürich, Switzerland*
[b]*Institute of Applied Physics, ETH Zürich, 8093 Zürich, Switzerland*
[c]*Institute of Particle Physics, ETH Zürich/Paul Scherrer Institute, Zürich, Switzerland*
[d]*Department of Electronic and Electrical Engineering, Loughborough University, Leicestershire, LE11 3TU, UK*

Abstract

The stability of CdTe/CdS solar cells depends on spatial changes of defects and impurities throughout the cell. Degradation effects are often associated with metal diffusion from the back contact of the cell, which is Cu in most cases. However, cells with stable back contact can also exhibit instability, as also all the other cell layers are potential sources of impurities causing instability. Cell degradation due to generation of defects from external influences like particle irradiation, e.g. in space, is another reason for instability. The development of stable back contacts as well as sources of instability in the cell performance are discussed with a special focus on the CdS layer and CdTe/CdS interface, which are very sensitive to the accumulation of impurities and defects. A non-destructive method to assess the stability issue is described. An analysis of performance stability with respect to defect generation caused by high-energy protons and electrons is presented. Additionally, effects of meta-stability and the capability to recover from degradation by defect relaxation are shown.

Keywords: Stability; CdTe; Irradiation; Thin films; Solar cells

1. Introduction

Performance of solar cells is always an important issue for terrestrial and space applications, which is widely studied also for CdTe/CdS solar cells. Most of the conventional CdTe solar cells use either Cu/Au or Cu/graphite for the back contact due to their initially beneficial effects on the performance. Yet, these cells usually show degradation, when stressed during long-term stability testing. One common assumption is that the diffusion of Cu into the CdTe absorber causes shunting, leading to a complete failure at the extreme. Hence, stability of CdTe solar cells is often considered predominantly a back contact issue. A variety of alternative back contacts have been already investigated and materials for stable contacts have been suggested.

Nevertheless, the stability of the solar cells is also determined by impurities originating from the source materials or processes. Those impurities can have strong and detrimental effects on the electronic properties of the cell, which can be especially observed in voltage-dependent quantum efficiency measurements, since this technique allows to distinguish effects in different cell layers, especially in CdS, by means of the spectral resolution [1,2].

Stability of solar cells is also a concern for their application in space, where the cells have to withstand high energy particles, mainly electrons and protons that can cause severe damage in solar cells up to a complete failure. The radiation hardness of the CdTe solar cells is presented and an explanation for the damage mechanism is given. Further, the damage recovery ability of the cells is shown.

2. Stable back contacts on CdTe/CdS solar cells

2.1. Experimental

The CdTe cells used for the development of a stable back contact consist of about 0.2-μm-thick CdS layer and about 6-μm-thick CdTe layer both deposited with close-spaced sublimation at ANTEC GmbH. The cells were activated in Cl vapour without oxygen prior to standard etching, in this case a mixture of nitric and phosphoric acid in water [3]. The back contact was

*Corresponding author. Tel.: +41-1-4451474; fax: +41-1-4451499.
E-mail address: tiwari@phys.ethz.ch (A.N. Tiwari).

0040-6090/04/$ - see front matter © 2003 Elsevier B.V. All rights reserved.
doi:10.1016/j.tsf.2003.10.141

Table 1
Overview of applied back contact material combinations

Metal	Buffer		
	Sb	Sb_2Te_3	Cu
Au	X	X	X
Mo	O	O	X
Al	X	X	

X indicates non-stable cells and O indicates stable cells.

subsequently deposited by physical vapour deposition of a variety of metals, semimetals or semiconductors in the sequence of a buffer layer followed by the metallisation (Table 1). Except for Sb_2Te_3, all layers were deposited at room temperature, whereas Sb_2Te_3 was deposited at a substrate temperature of 150 °C. This temperature is sufficient to allow for a congruent deposition of stoichiometric Sb_2Te_3, while lower temperatures result in deposition of different phases, especially when other deposition methods like sputtering are used [4].

In case of the reference back contact, i.e. Cu/Au, a post-deposition annealing in air at 200 °C for 30 min is required to obtain the best performances. This is explained by the diffusion of Cu into the absorber and the formation of $Cu_{2-x}Te$ at the interface, allowing for an quasi-ohmic back contact. This final back contact annealing may not be required for back contacts without Cu.

All standard devices yielded initial efficiencies in the range of 9–12%. Cells with Cu/Au contacts show typically ~1% higher efficiency than cells with Sb/Mo or Sb_2Te_3/Mo contacts, due to a barrier formation at these back contacts.

2.2. Stability testing

The cells underwent two main methods of stability testing. The first test was an annealing at 200 °C for 30 min in air subsequent to previous standard processing methods. This temperature enables back contact materials to diffuse into the absorber and degrade the electronic properties of the back contact. Fig. 1 shows the efficiencies for a variety of back contact combinations. Solid squares represent the initial efficiencies and open triangles with central dots represent efficiencies after stressing. Performance degradation occurs for cells with Al, Au or Cu at the back contact, while cells with Mo metallisation do not degrade when a buffer layer of Sb or Sb_2Te_3 is applied.

The second test is an accelerated life time test using a climate chamber where the cells are kept at 65 °C cell temperature in air at 1 sun illumination in open circuit conditions. The results for this 'light soaking' test are quite similar to the results of the annealing test. Only cells with a Mo metallisation and buffers of Sb and

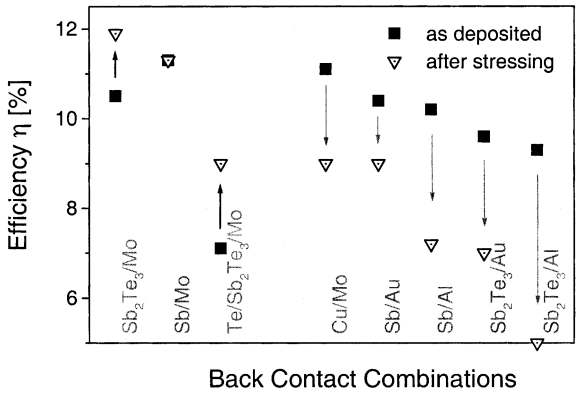

Fig. 1. Efficiencies of CdTe cells with different back contacts in as-deposited conditions and after annealing at 200 °C. Contacts containing fast diffuser impurities (Cu, Al, Au; right part of graph) degraded severely.

Sb_2Te_3, respectively, show non-degrading long-term performance with negligible meta-stability effects [5].

The cause of degradation for the other cells is the diffusion of back contact materials into the absorber as is observed by secondary ion mass spectroscopy (SIMS) measurements (Fig. 2). The diffused impurities tend to accumulate in CdS and at the front contact CdS/TCO interface. They change the electrical properties of the junction and lead to shunting in the extreme case.

The two candidates for a stable back contact, Sb/Mo and Sb_2Te_3/Mo, the latter first investigated by Romeo et al. [6], were tested more rigorously at 80 °C cell temperature for a much longer time period. On the basis of an evaluation of Hiltner and Sites [7], we assume for this stressing condition a moderate acceleration factor of 100. The results are shown in Fig. 3. The efficiencies of the cells with Sb_2Te_3/Mo back contact increased during the first 5 months of testing by approximately 10% relative. This can be attributed to a light soaking

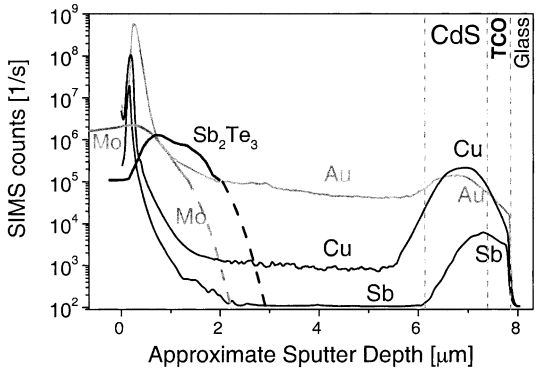

Fig. 2. SIMS profiles for cells with different back contacts, overlapped in one graph for better comparison. Cu and Au diffuse into the absorber accumulating in CdS and at the front contact of the cell. This applies also to a minor extent to Sb; however, no diffusion of Sb from an Sb_2Te_3 buffer or of Mo is detectable.

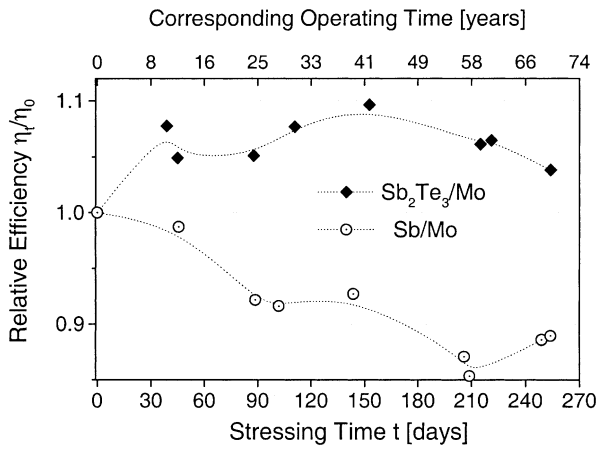

Fig. 3. Light soaking of cells with Mo metallisation and Sb or Sb_2Te_3 buffers at 80 °C. Cells with Sb_2Te_3 buffers exhibited an efficiency increase in the beginning. Cells with Sb buffers lost some efficiency that is partly explained by contact oxidation during stressing in air.

effect and changes at the back contact interface facilitating a better contact, which is supported by the analysis of the *I–V* characteristics. Upon further testing, the cells exhibit a slow drop in efficiency. After 9 months of testing the cells are still 4% (relative) above their initial efficiency. Since the 'bare' cells are tested in air, the slight decrease of efficiency in the later testing phase is mainly caused by oxidation of the contacts and can be avoided with a proper encapsulation.

The situation is different for cells with Sb/Mo back contacts where about 8% (relative) degradation in the first 5 months of testing is observed and the cells have gone a degradation of 11% (relative) after 9 months of testing. The testing time of 9 months corresponds with the acceleration factor of 100 to an outdoor operation time of more than 70 years.

The performance degradation of Sb/Mo contacted cells is caused again by the oxidation of the back contact and by the increase of a barrier, as is determined from *I–V* characteristics. A part of this barrier is present at the back contact; however, there is also a light modulated barrier (LMB) at the pn-junction or in the CdS, which becomes more evident when impurities change the properties of the CdS; compare also SIMS measurements shown in Fig. 2. This is explained in more detail in the following section.

By choosing the right buffer–metal combination, stable CdTe solar cells are obtained. Cells with a Sb_2Te_3/Mo buffer show excellent stability and stress tests suggest that these cells will not degrade when properly encapsulated. Although cells with Sb/Mo back contacts show a small degradation, they might be still considered to be sufficiently stable for standard application. Furthermore, this back contact combination might also be interesting for production, since it is cheaper and easier to process.

3. Influence of impurities and electrical characterisation

3.1. Experimental

Although there is a strong dependence of the stability on the back contact material, but this may not be the only source of cell degradation. In general, any kind of impurity incorporated during processing can influence the performance stability. Fig. 4 shows the efficiency trends of cells with CdTe absorbers from consecutive depositions and stable Sb/Mo back contacts. Even though these cells have not been stressed, like in the case of life time testing, they exhibit degradation even when stored in the dark, with a clear dependence on the deposition sequence, i.e. cells with absorbers from the first deposition degrade much faster than those from the last deposition. A probable reason is impurities originating either from the source material, in this case they are fast evaporating contaminations in the source material, or from the processing itself, e.g. contamination in the deposition apparatus. Of further interest are the initial efficiencies depending on the impurities as well. In the beginning the impurities facilitate a higher efficiency accompanied, however, by severe degradation that meets the trend for cells containing Cu in the back contact.

Presently, little is known about the requirements for source material with respect to purity to produce highly efficient and stable CdTe cells. Investigations on source material impurities have been done by means of SIMS analysis [8]. However, it has not yet been specified how detrimental specific impurities are and what is the minimum acceptable concentration.

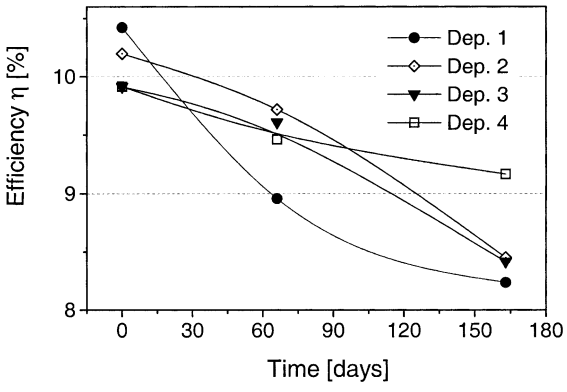

Fig. 4. Degradation of CdTe/CdS cells with consecutively deposited CdS/CdTe layers and identical Sb/Mo back contacts. The cells were stored at room temperature omitting extra stressing.

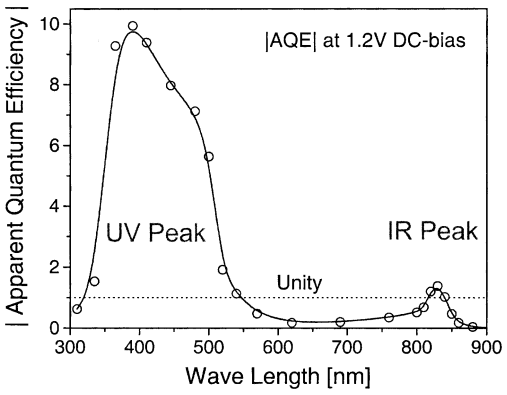

Fig. 5. Typical AQE of a CdTe/CdS solar cell at forward bias of approximately 1 V. There is a large gain-peak in the spectral range of CdS absorption and a smaller gain-peak in the spectral region near the CdTe band edge.

3.2. Impurities in CdS and the light modulated barrier

The CdS layer is particularly sensitive to impurity incorporation. Some impurities can create deep defect levels in CdS, which can have very asymmetric capture cross-sections for electrons and holes. Thus, they act as traps in the dark but as recombination centres under illumination. The net carrier density under illumination is changed by a so-called electronic doping, allowing for changes in conductivity and even type behaviour [9,2]. The consequence for CdTe solar cells is the existence of an LMB in CdS, i.e. a barrier in CdS being higher in the dark due to carrier trapping and lower under illumination due to the electronic doping [9]. The effects of this LMB are most visible in quantum efficiency measurements under applied bias, the so-called apparent quantum efficiency (AQE). Under forward bias the modulation of the barrier during the AQE measurement causes a secondary photo current, which is rather determined by the bias than by the absorbed photons. This enables a current gain which is observed in AQE signals well above unity mainly in the spectral range where CdS absorbs, i.e. below 515 nm. Similar effects can stem from the barrier in the back contact, which is sensitive in the spectral region near the absorption edge of CdTe, i.e. from 800 to 850 nm (Fig. 5).

3.3. Impurity diffusion monitoring by AQE

Using the AQE characterisation method which enables the qualitative monitoring of the LMB, cells with back contacts of Cu/Au and Sb/Mo have been investigated. The back contact served as the source of impurities that are intentionally diffused into the CdTe absorber and cell by annealing processes carried out in air and in vacuum at temperatures of 250 °C for 45 min. With this non-destructive approach, the role of oxygen on the diffusion of different elements could be monitored as well. Standard lock-in-technique was used to measure the AQE in the range of 300–1050 nm using a grid-monochromator without additional bias illumination. A custom-made trans-impedance-amplifier was used to apply bias voltage in order to keep the cell at the adjusted work point while signal and phase have been measured.

Cells with a back contact of a 6-nm Cu buffer layer and a 50-nm Au metallisation degraded to approximately 7% efficiency from initial efficiency of approximately 11%, when stressed in air at 250 °C. Further stressing at 300 °C in air decreases efficiency to below 0.5%. The general trend of degradation is shunting and an increase in series resistance. After the second annealing at 300 °C, the photo-generated current has dropped dramatically, indicating a severe damage of the photovoltaic junction, suggesting very weak carrier collection due to recombination losses. Cells with the same Cu/Au back contact were also stressed in vacuum at 250 °C. The stressing degradation in air and in vacuum is roughly the same with a somewhat stronger degradation for the vacuum stressing to below 6% efficiency. A difference might originate to some extent from different furnace temperatures.

The degradation cause is indicated by the decrease in diffusion length L_{eff} as determined from the QEs (at 0 V). The decrease in L_{eff} likely arises from newly formed recombination centres originating from diffused impurities.

For clarity of presentation here, the described measurements are restricted to the AQE of one wavelength in the region of the blue response peak, i.e. at 410 nm as a function of bias. The AQEs for Cu/Au and Sb/Mo back contacted cells are shown in Fig. 6 for non-, air- and vacuum-stressed cells. The AQEs of the Cu/Au back contacted cells (open symbols) all exceed unity in a medium bias range approximately 0.8 V. At approximately 1.2 V bias the differences in the AQEs for

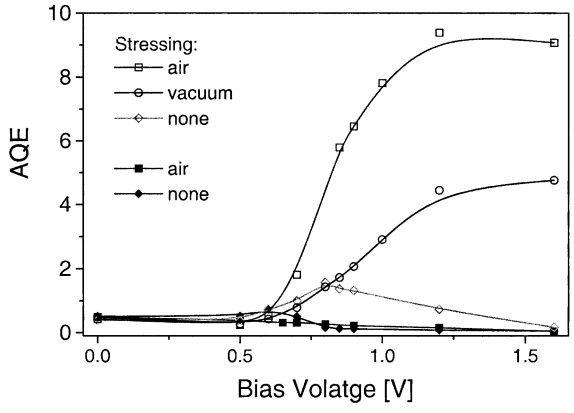

Fig. 6. Bias-dependent AQE at 410 nm. Open symbols refer to Cu/Au contacted cells, solid symbols refer to Sb/Mo contacted cells. The AQE gain differs significantly with the back contact.

different stressing are most obvious; the stressed cells show a higher AQE gain than the non-stressed reference. The AQE gain for air-stressed cells is approximately two times larger than that for vacuum-stressed cells. According to the model the LMB is increased by stressing. In the presence of oxygen the LMB is significantly more increased than that in the absence of oxygen. The AQE graph in Fig. 6 shows a maximum, when the forward bias starts to override the LMB modulation.

A completely different degradation pattern is seen for cells with Sb/Mo contacts, also shown in Fig. 6 (solid symbols). Both AQE characteristics for non- and air-stressed cells stay below unity. While the non-stressed cells exhibit a small gain in AQE of approximately 0.7 V, the air-stressed cells show no AQE peak. This supposes that the LMB is lowered to an extent where no AQE gain is achieved any more.

A similar analysis of the AQEs in the near infra-red region comes to a consistent conclusion. Since AQE gains are only observed in case of air-stressing, more pronounced in Cu/Au contacted cells than that in Sb/Mo contacted cells, a back contact barrier increase by oxidation is presumed [10].

Together with the SIMS profiling and accelerated lifetime testing, the most plausible cause of degradation of the cells with Cu/Au back contact is the diffusion of Cu and Au along the grain boundaries into the CdS where it accumulates. Since Cu and Au act as acceptors in CdS, they are causing or increasing the donor-compensation, thus creating the LMB by introduction of a barrier in the conduction band in CdS. These acceptors are also effective recombination centres under illumination, because of their typical mid-gap location in CdS. The Sb/Mo cells exhibit a decrease of the LMB after stressing since no gain in the AQE occurs. This suggests that there is no diffusion of Sb or Mo of any electrical relevance from the back contact into CdS. If there should be diffusion of Sb into CdS at all, there must not be a donor-compensation effect since the barrier gets lowered; additionally, diffusion is expected to be much slower due to the larger atomic radius of Sb compared to Cu. An effect of oxygen on the LMB can be neglected, since the Sb/Mo contacted cells have been stressed in air and exhibit no AQE peak. Additionally, oxygen can act as donor in CdS [11], which will decrease the LMB. This suggests that oxygen promotes the Cu diffusion into CdS but is not diffusing as oxygen into CdS, which was already presumed earlier [12].

4. Stability with respect to particle irradiation

When solar cells are used in space for power generation, the main concern is the degradation due to damage caused by high energy particles like electrons and protons. The damage determining parameter is the material-dependent non-ionisation energy loss (NIEL) of the particles penetrating into the cell [13]. For protons, the NIEL is higher for lower energies (above a threshold energy), whereas for electrons, the NIEL increases with energies. The penetration depth of the particles depends upon their energy, cross-sections with the stopping atoms and target material density. It is much smaller for protons than that for electrons. The NIEL, in combination with particle penetration and the fluence, determines the damage relevant for the photovoltaic properties.

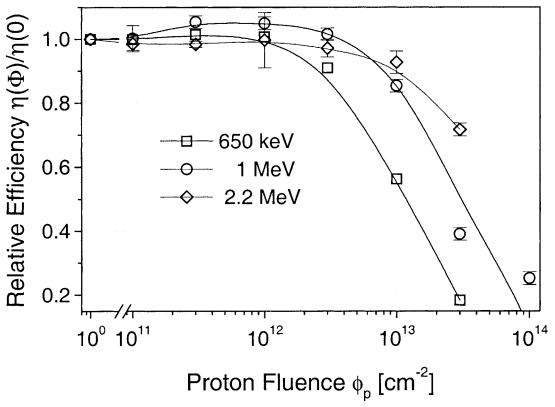

Fig. 7. Relative efficiencies of the irradiated CdTe cells as a function of the proton fluence.

To test the radiation hardness of CdTe/CdS solar cells developed at ETH Zurich, they were irradiated with protons of 0.65, 1 and 2.2 MeV, and fluences ranging from 10^{11} to 10^{14} cm^{-2}, as well as with high energy electrons of 1 and 3 MeV with very high fluences between 2×10^{16} to 8×10^{17} cm^{-2}. Proton irradiation was performed at the PSI/ETHZ TANDEM accelerator at the Institute of Particle Physics of the Swiss Federal Institute of Technology Zurich (ETHZ). Electron irradiation was performed at the DYNAMITRON electron accelerator at the Institute of Radiation Physics in collaboration with the Institute of Physical Electronics (IPE) of the University of Stuttgart [14]. The cells were irradiated on the uncovered back sides with a perpendicular, monochromatic beam directly incident on the cell layers, thus avoiding inaccuracy due to a spectral shift towards a lower energy polychromatic spectrum caused by the glass. The influence of the 40-nm thin back contact layers (Cu/Au) upon the particle energy is negligible under the chosen conditions, having even less effect than a TCO or an anti-reflection coating.

The performance change of irradiated cells depends on proton energy and fluence, as shown in Fig. 7, which displays the relative efficiency vs. the proton fluence for three different energies. The protons of 650 keV are most damaging, whereas less damage is caused by 1 and 2.2 MeV protons. This is consistent with the NIEL estimates. The proton irradiation has no effect on the

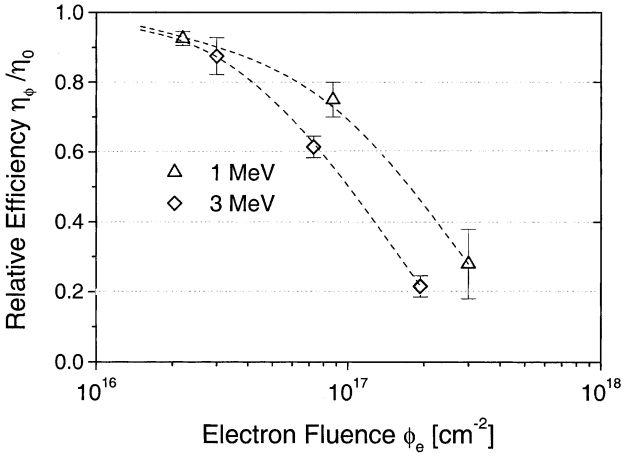

Fig. 8. Efficiency–fluence characteristics of electron irradiated CdTe solar cells.

efficiencies for low fluences up to 10^{11} cm^{-2}. At medium fluences (10^{12} cm^{-2}) a slight increase is observed, which is largest for 1-MeV protons. At high fluence of $1–3\times10^{12}$ cm^{-2} and depending on the energy, the onset of degradation starts. The possible efficiency increase for medium fluences is caused by an increase in V_{OC} of up to 20 mV, which is nearly independent of proton energy. This increase is supposedly caused by a passivation of recombination centres invoked by the ion implantation (hydrogen in case of protons). At higher fluences, the V_{OC} starts to decrease with a strong dependence on proton energy. The current density J_{SC} remains practically unchanged up to fluences of 3×10^{12} cm^{-2}. The main cause for the decrease in efficiency at higher fluences is the loss in J_{SC}. Quantum efficiency measurements exhibit a decrease of the near infra-red response for cells with decreased J_{SC}, indicating a shorter effective diffusion length [15]. This suggests an increase in the recombination centre density.

The V_{OC} and FF of the electron irradiated cells are only weakly affected under these extremely damaging conditions. The V_{OC} and FF exhibited a decrease to 85% of the pre-irradiation value after the most damaging irradiation. The efficiency-fluence characteristics shown in Fig. 8 are dominated by the decrease of J_{SC}, an effect that is even more pronounced than that in the case of proton irradiation. It should be noted that such extreme conditions are seldom encountered in space and usually cause a complete failure of crystalline Si solar cells.

The formalism of the displacement damage dose (DD) developed by Summers and coworkers (NRL, USA) allows a comprehensive way to predict irradiation damage for a given cell technology and compare it to other technologies [16]. The particle fluence is converted into DD by the multiplication with the material-specific NIEL. This allows the depiction of the efficiency-DD characteristics. When depicted as a function of DD, the relative efficiencies for all energies coincide to a single degradation characteristic, one for protons and one for electrons. By scaling with a characteristic factor for each cell technology, the degradation characteristics for electrons and protons coincide to a single master degradation curve [16]. A comparison of the degradation curve for CdTe/CdS cells [14] to the curves of other cell technologies [17] is shown in Fig. 9. The CdTe/CdS cells exhibit a superior radiation hardness over the other cell technologies. At very high doses the degradation of CdTe cells seems to get worse than those of the other cells; however, the testing of cell stops at such extreme doses, therefore a simple extrapolation of the degradation behaviour is inappropriate [17]. Moreover, such irradiation conditions (very high fluences and defect introduction rates) are rarely encountered in space, as it would require many years for the collection of such doses.

The performance recovery of CdTe cells was monitored for samples stored at room temperature in the dark, even though the recovery should be faster at elevated temperatures and/or illumination. A fast recovery of all irradiated cells is observed already at room temperature. The time dependence of this recovery allowed the determination of a recovery rate. For electron irradiated cells the recovery rate was determined to be independent of electron fluence and energy [14], which indicates a homogenous damage and recovery following the same mechanism. The time after which half of the damage is recovered is determined to be approximately 12 days in the above mentioned conditions. Due to this fast recovery of the cells, the actual damage apparent in space would be considerably less or even nonexistent, because the collection of damaging doses might require up to several years.

The analysis of the damage caused by protons was performed with a Monte Carlo simulation using the

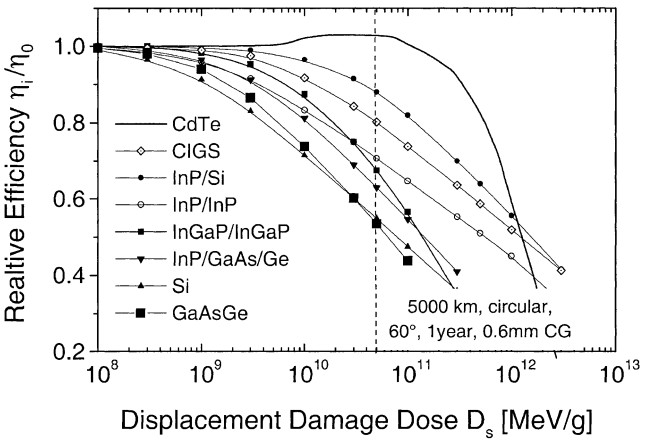

Fig. 9. Degradation curves of different solar cells. Data, except for CdTe, are taken from Ref. [17].

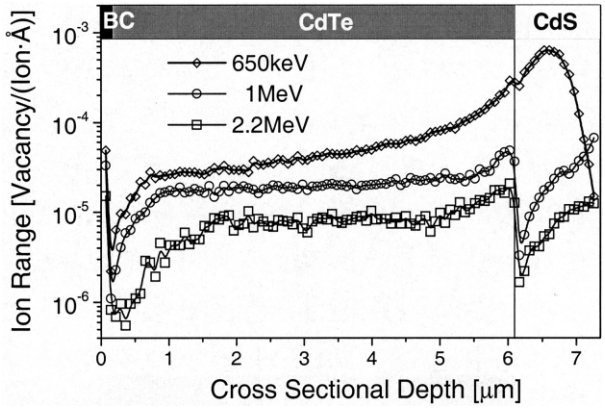

Fig. 10. Simulation of the generated vacancy profile in the irradiated CdTe cells for different proton energies.

computer program that calculates the stopping and range of ions in matter [18]. The simulation derived a cross-sectional profile of vacancies generated by protons of different energy in the layer stack of the actually used CdTe cells (Fig. 10). The profile shows approximately two orders of magnitude higher vacancy density at the CdTe/CdS interface (the pn-junction) for 0.65-MeV protons compared to the higher energy protons. The simulation yields an almost complete absorption of 0.65-MeV protons in the cell, i.e. all energy is lost in the cell layers, whereas for energies of 1 MeV and above more than 99% of the protons are transmitted losing much of their energy in the cell structure. The remaining kinetic energy would be most damaging when stopping takes place in the cell layers. This explains why the 0.65-MeV protons are most damaging to the tested cells. With the knowledge of the cross-sectional damage profile, a further optimization of the cell design for a specific application, e.g. a special space mission, is possible.

5. Conclusions

Stable CdTe/CdS solar cells are obtained by applying an Sb_2Te_3/Mo back contact. Cells with an Sb/Mo back contact have a slightly inferior stability. However, for industrial production the application of an Sb buffer would be preferred over an Sb_2Te_3 buffer because of lower cost and less stringent process control requirements. Material impurities from other sources are also a concern for the stability of the solar cells. SIMS measurements revealed the accumulation of impurities in the CdS layer where they have a strong impact on the electrical properties of the cell by influencing a naturally existing barrier in the CdS. These effects of impurity diffusion on the electrical properties were investigated by means of the AQE characterisation, which provides a non-destructive method to obtain spatial information linked to the electrical phenomena in CdTe cells.

The AQE measurements in conjunction with SIMS profiles indicated the enhanced diffusion of Cu and its accumulation in the CdS layer due to annealing in air. A similar effect for Sb/Mo back contacted cells was not found.

For space application CdTe/CdS solar cells exhibit an excellent stability under high energy particle irradiation. The onset of cell degradation typically occurs at particle fluences, which are two orders of magnitude higher than that conventionally used for monocrystalline space solar cells of Si or III–V compounds. The degradation mechanism is explained by the generation and passivation of recombination centres by the particles. Since the cells show a fast recovery from the introduced damage, presumably due to the strong defect compensation effects in CdTe, there is little or no damage to be expected for standard space applications. Using the displacement DD approach a degradation master curve is obtained, which allows for easy comparison to other cell technologies and calculation of solar array requirements for a given space mission.

Acknowledgments

A part of this work was performed within the CADBACK project of the European JOULE program and supported by the Swiss Office of Education and Science. D. Bonnet, M. Campo and J. Beier from ANTEC GmbH are kindly acknowledged for the supply of CdTe/CdS samples for back contacting. M.G. Burri and G. Troillet from the Universite de Lausanne are thanked for the SIMS-measurement. A. Jasensek, K. Weinert and U. Rau from the Institute of Physical Electronics (IPE) at the University Stuttgart are thanked for electron irradiation.

References

[1] D.L. Bätzner, G. Agostinelli, A. Romeo, H. Zogg, A.N. Tiwari, MRS Proc. 668 (2001) H5.17.
[2] M. Köntges, R. Reineke-Koch, P. Nollet, J. Beier, R. Schäffler, J. Parisi, Thin Solid Films 403–404 (2002) 280–286.
[3] D.L. Bätzner, R. Wendt, A. Romeo, H. Zogg, A.N. Tiwari, Thin Solid Films 361–362 (2000) 463–467.
[4] A.E. Abken, O.J. Bartelt, Thin Solid Films 403–404 (2002) 216–222.
[5] D.L. Bätzner, A. Romeo, R. Wendt, H. Zogg, A.N. Tiwari, Thin Solid Films 387 (2001) 151–154.
[6] N. Romeo, A. Bosio, R. Tedeschi, A. Romeo, V. Canevari, Solar Energy Mater. Solar Cells 58 (2) (1999) 209–218.
[7] J.F. Hiltner, J.R. Sites, National Center for Photovoltaics 15th Program Review Meeting, AIP Conference Proceedings 462 (1999) 170–173.
[8] K. Durose, D. Boyle, A. Abken, C.J. Ottley, P. Nollet, S. Degrave, M. Burgelman, R. Wendt, J. Beier, D. Bonnet, Phys. Status Solid B 229 (2) (2002) 1055–1064.
[9] G. Agostinelli, E.D. Dunlop, D.L. Bätzner, A.N. Tiwari, P. Nollet, M. Burgelmann, M. Köntges, Proceedings of the Third

World Conference on Photovoltaic Energy Conversion, Osaka, in press.
[10] D.L. Bätzner, G. Agostinelli, M. Campo, A. Romeo, J. Beier, H. Zogg, A.N. Tiwari, Thin Solid Films 431–432 (2003) 421–425.
[11] R.H. Bube, Photoelectronic Properties of Semiconductors, Cambridge Press, 1992, Chapter 2.
[12] K.D. Dobson, I. Visoly-Fischer, R. Jayakrishnan, K. Gartsman, G. Hodes, D. Cahen, MRS Symp. Proc. 668 (2001) H8.24.
[13] S.R. Messenger, E.A. Burke, G.P. Summers, M.A. Xapsos, R.J. Walters, E.M. Jackson, B.D. Weaver, IEEE Trans. Nucl. Sci. 46 (6) (1999) 1595–1602.
[14] D.L. Bätzner, A. Romeo, M. Döbeli, K. Weinert, H. Zogg, A.N. Tiwari, Proceedings of 29th IEEE PVSEC (2002) 982–985.
[15] D.L. Bätzner, A. Romeo, H. Zogg, A.N. Tiwari, Proceedings of 17th European Photovoltaic Solar Energy Conference (2001) 1043–1046.
[16] S.R. Messenger, G.P. Summers, E.A. Burke, R.J. Walters, M.A. Xapsos, Prog. Photovoltaics 9 (2001) 103–121.
[17] G.P. Summers, S.R. Messenger, Tutorial #2, 29th IEEE PVSEC (2002).
[18] J.E Ziegler, J.P. Biersack, U. Littmark, The Stopping and Range of Ions in Solids, Pergamon Press (1985) ISBN: 0-08-021603-X.